Chinese Chemical Letters 35 (2024) 108825

Contents lists available at ScienceDirect

Chinese Chemical Letters

journal homepage: www.elsevier.com/locate/cclet

Design, synthesis and biological evaluation of fluorescent derivatives of ursolic acid in living cells

Wenyi Mei[a,1], Lijuan Xie[a,1], Xiaodong Zhang[a], Cunjian Shi[a], Fengzhi Wang[a], Qiqi Fu[a], Zhenjiang Zhao[a], Honglin Li[a,b,c,*], Yufang Xu[a,*], Zhuo Chen[a,*]

[a] Shanghai Key Laboratory of New Drug Design, State Key Laboratory of Bioreactor Engineering, School of Pharmacy, East China University of Science and Technology, Shanghai 200237, China
[b] Innovation Center for AI and Drug Discovery, East China Normal University, Shanghai 200062, China
[c] Lingang Laboratory, Shanghai 200031, China

ARTICLE INFO

Article history:
Received 9 May 2023
Revised 17 July 2023
Accepted 18 July 2023
Available online 20 July 2023

Keywords:
Pentacyclic triterpenoid
Ursolic acid
Fluorescent derivatives
Autophagy
Apoptosis

ABSTRACT

Ursolic acid (UA) is a naturally occurring ursane triterpenoid, which exhibits a wide range of unique biological activities. To clarify its mechanism of action (MOA), a series of fluorescent derivatives of UA (**5a**–**c**) were designed and synthesized by conjugation with 7-nitrobenzo-2-oxa-1,3-diazole (NBD) fluorophore. Among them, **5c** exhibited similar anti-proliferative activity with UA against HCT116 cells (half maximal inhibitory concentration (IC_{50}) = 9.21 ± 0.50 μmol/L). Cell imaging experiment indicated that **5c** was rapidly taken up in HCT116 cells in a dose and time-dependent manner. Then, **5c** was found to localize in endoplasmic reticulum (ER), lysosomes, and mitochondria, but not in nucleus of HCT116 cells by confocal microscopy studies. Preliminary MOA proved that UA induced autophagy with a unique intracellular distribution mechanism involving ER and lysosome. In all, our work provides new clues for revealing the molecular mechanism of UA as an antitumor agent.

Ursolic acid (UA, Fig. 1A) is widespread in fruits, vegetables, and medicinal herbs. It has attracted considerable attention due to its remarkable pharmacological activities, such as anti-inflammatory [1,2], antiviral [3–5], hepatoprotective [6,7]. It has also shown efficacy in treating solid tumors, including gallbladder carcinoma, breast cancer, and colorectal cancer [8–10]. UA is an interesting and important natural triterpenoid for cancer therapy, but it faces several challenges, including poor water solubility, poor pharmacokinetic properties, and unclear mechanism of action [11–13].

UA was reported to inhibit colorectal cancer (CRC) tumor growth and metastasis alone or in combination with other antitumor agents [14–16]. For example, UA synergized with oxaliplatin and inhibited CRC cell proliferation and tumor growth *in vivo* [14]. Given the significant potential of UA in cancer prevention and treatment, its detailed mechanism of action needs in-depth exploration. Recently, various technological and scientific developments have been employed to elucidate the actions of bioactive natural products, including biochip technology, drug affinity responsive target stability (DARTS), and activity-based protein profiling (ABPP). Among them, fluorescence imaging technology showed its advantages due to high sensitivity, fast response speed, *in situ* detection in living cells, practicality, and simplicity of operation [17]. Therefore, fluorescence imaging technology is widely used to investigate cellular uptake, cellular localization, and specific interactions associated phenotypes of bioactive natural products in living cells [18–26].

To date, the distribution of UA in cells has not been reported. Therefore, in this study, we designed and synthesized novel fluorescent derivatives based on UA to visualize their cellular uptake and subcellular localization.

The fluorescent derivatives were designed by UA combined with a fluorophore *via* a linker region. Firstly, UA should be derived from a position with minimal influence on its pharmacological profile. UA exhibited potent antiproliferative activity against HCT116 cells with half maximal inhibitory concentration (IC_{50}) value of 8.75 ± 0.13 μmol/L (Table 1). Replacement of 3β-OH with hydroxamic acid (UA-1) resulted in a slight loss of cytotoxicity (IC_{50} = 26.49 μmol/L, Table S1 and Fig. S1 in Supporting information). Furthermore, structural modifications of 3β-OH with acetylation (UA-2) and dichloroacetate (UA-3), resulted in complete loss of against HCT116 cells activity (IC_{50} > 50 μmol/L, Table S1 and

* Corresponding authors.
E-mail addresses: hlli@ecust.edu.cn (H. Li), yfxu@ecust.edu.cn (Y. Xu), chenzhuo@ecust.edu.cn (Z. Chen).
[1] These authors contributed equally to this work.

https://doi.org/10.1016/j.cclet.2023.108825
1001-8417/

Table 1
Antiproliferative activities of **5a–c** and NBD-C6-NH_2.

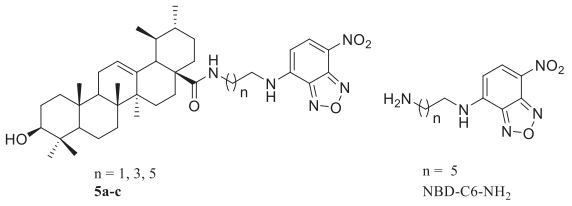

Compd.	*n*	HCT116 IC_{50} (μmol/L)[a]
UA	–	8.75 ± 0.13
5a	1	>50
5b	3	>50
5c	5	9.21 ± 0.50
NBD-C6-NH_2	5	>50

[a] CCK-8 assays: HCT116 cells were incubated with compounds for 72 h (means ± standard deviation (SD), $n = 3$).

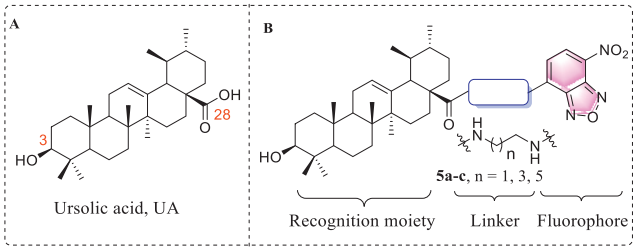

Fig. 1. Design fluorescent derivatives of UA. (A) Chemical structure of UA. (B) Fluorescent derivatives design strategy based on UA.

Fig. S1). Therefore, 3β-OH was important for the antiproliferative activity against HCT116 cells. We selected C-28 carboxyl group for conjugating reactions. Secondly, 7-nitro-2,1,3-benzoxadiazole (NBD) was then selected as fluorophore due to its excellent fluorescence/pharmacological properties, such as water solubility, small size, cell permeability, and low toxicity [27]. Lastly, the conjugation strategies were important for development of fluorescent derivatives [28]. Thus, the carboxyl group of UA was extended by an alkyl linker and subsequently connected with NBD, affording three UA fluorescent derivatives (**5a–c**, Fig. 1B).

The antiproliferative activities of **5a–c** (Fig. S2 in Supporting information) was evaluated *in vitro* in comparison with UA. As shown in Table 1, no obvious antiproliferative activities was detected for compounds **5a** and **5b** with two or four-carbon spacers (IC_{50} > 50 μmol/L). The fluorescent derivatives with six-carbon spacers (**5c**) exhibits cytotoxicity equivalent to that of UA against HCT116 cells. NBD-C6-NH_2 with no UA moiety (Fig. S3 in Supporting information) has no antiproliferative activity on HCT116 cells (IC_{50} > 50 μmol/L). Considering the favorable antiproliferative activity of **5c**, it was selected for subcellular localization studies. As shown in Fig. S4 (Supporting information), **5c** exhibits significant differences between maximum absorption (λabs = 480 nm) and emission (λem = 540 nm) wavelengths with a large stokes shift of 60 nm in an aqueous solution, which was suitable for the imaging studies.

To further investigate the uptake of **5c** by HCT116 cells using fluorescence microscopy, the dose dependence and time dependence of **5c** in HCT116 cells were tested. As shown in Fig. 2A, bright green fluorescence staining was observed inside the HCT116 cells when **5c** was incubated at a concentration of 5, 10, and 20 μmol/L for 1 h, indicating that **5c** could enter HCT116 cells in a concentration-dependent manner. Similarly, **5c** began to be absorbed into HCT116 cells after 15 min of incubation (Fig. 2B), indicating that the uptake of **5c** at this concentration is quick and in time-dependent manner.

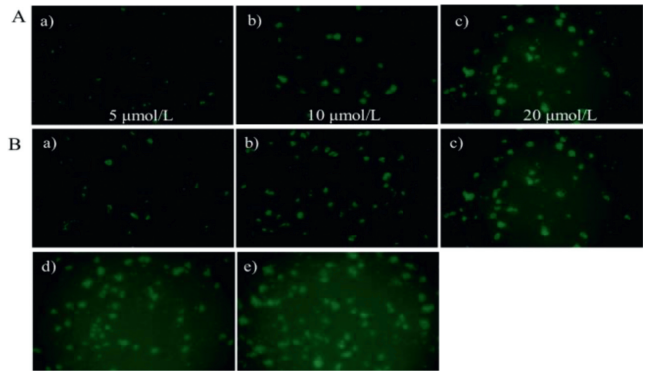

Fig. 2. The uptake of indicated **5c** in HCT116 cells, images were collected using fluorescence microscopy. (A) The dose-course uptake of 20 μmol/L **5c** in HCT116 cells, (a) 5 μmol/L **5c** for 1 h, (b) 10 μmol/L **5c** for 1 h, (c) 20 μmol/L **5c** for 1 h. (B) The time-course uptake of 20 μmol/L **5c** in HCT116 cells, (a) HCT116 cells were treated with 20 μmol/L **5c** for 0.25 h, (b) 0.5 h, (c) 1 h, (d) 2 h, (e) 4 h. Enlarged view of representative cells, 10×.

To further investigate the subcellular localization of UA, we treated **5c** in HCT116 cells with various organelle-specific dyes. As shown in Fig. 3, confocal microscopy of HCT116 cells contained with LysoTracker Red, ER Tracker, and Mito Tracker confirmed the localization of **5c** in lysosomes, ER, and mitochondria with a Pearson's correlation coefficient (PCC) value of 0.88, 0.92, and 0.70, respectively. In contrast, **5c** exhibited almost no colocalization in nucleus (Fig. S5 in Supporting information). Additionally, when we tested NBD-C6-NH_2, no obvious overlap was detected (Fig. S6 in Supporting information). Therefore, **5c** provided visual evidence that UA primarily localized with mitochondria, lysosome, and ER in living cells.

The mitochondrion plays a critical role in apoptosis, while lysosomes and ER play critical roles in autophagy [29–32]. Previous reports have indicated that UA induced apoptosis and autophagy in various cancer cells, such as T47D, MCF-7, and PC-3 cells [33,34]. Our subcellular localization studies have shown that UA was distributed in the mitochondrion, ER, and lysosomes in HCT116 cells. To further clarify the subcellular distribution of UA and its regulation of cell function, we investigated the expression levels of apoptosis- and autophagy-related proteins by Western blot. UA could down-regulate the expression levels of caspase-3 and poly ADP-ribose polymerase (PARP) in a concentration-dependent manner. Additionally, the expression levels of cleaved caspase-3, cleaved PARP, and p53 were up-regulated in a concentration-dependent manner after incubation with UA for 24 h (Fig. S7A in Supporting information). Moreover, the expression levels of LC3-I, LC3-II, and p62 were up-regulated with increasing the concentrations of UA, and the ratio between LC3-II and LC3-I also increased (Figs. S7B and C in Supporting information). These results indicate that UA was widespread distributed in the ER, lysosome, and mitochondria and exert its effects through autophagy and apoptosis mechanisms.

In summary, we designed and synthesized three fluorescent UA derivatives with a large stokes shift. Luckily, **5c** retained similar antitumor activity with UA against HCT116 cells using cell counting kit-8 (CCK-8) assays *in vitro*, with IC_{50} value of 9.21 ± 0.50 μmol/L. Fluorescence microscopy studies confirmed that **5c** could quickly transport into HCT116 cells in a concentration- and time-dependent manner. Confocal microscopy experiments revealed that **5c** was distributed in the ER, lysosomes, and mitochondrial. Inspired by subcellular localization study, the involvement of autophagy and apoptosis mechanisms was demonstrated through

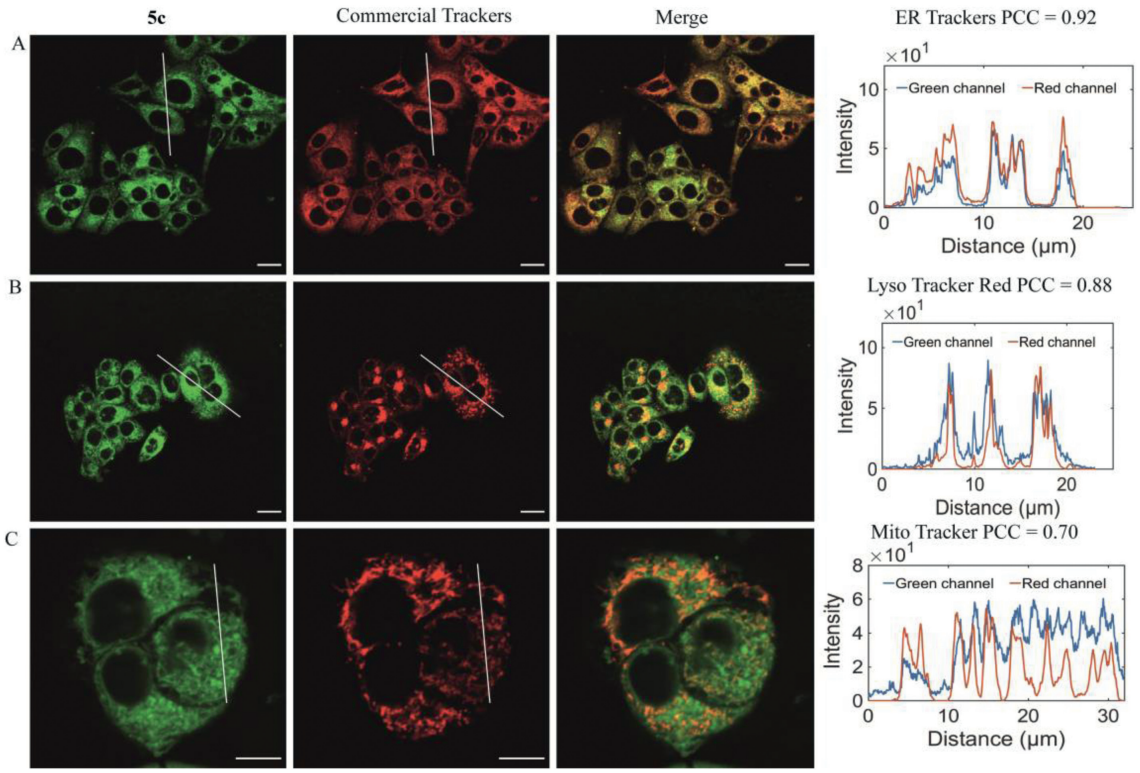

Fig. 3. Subcellular localization of **5c**. (A) Subcellular localization of **5c** and ER Tracker (ER specific dye) in HCT116 cells. HCT116 cells incubated with 20 μmol/L **5c** for 1 h. ER tracker at λex = 587 nm and λem = 615 nm. (B) Subcellular localization of **5c** and LysoTracker (lysosomes specific dye) in HCT116 cells. HCT116 cells incubated with 20 μmol/L **5c** for 1 h. LysoTracker Red at λex = 577 nm and λem = 590 nm. (C) Subcellular localization of **5c** and Mito Tracker (mitochondria specific dye) in HCT116 cells. HCT116 cells incubated with 20 μmol/L **5c** for 1 h. Mito Tracker at λex = 579 nm and λem = 599 nm. Scale bar: 20 μm. Images were collected by confocal microscopy (Nikon A1R).

Western blot analysis. Overall, our work provides deeper insights and visual tool for further studying the mechanisms in living cell.

Declaration of competing interest

The authors declare that they have no known competing financial interests or personal relationships that could have appeared to influence the work reported in this paper.

Acknowledgments

The research is supported in part by the National Key Research and Development Program of China (No. 2022YFC3400501), the National Natural Science Foundation of China (Nos. 81825020 and 82150208 to H.L.), the Shanghai Science and Technology Commission Biomedical Science and Technology Support Special Project (Nos. 21S11907900 and 20S11901000 to Z.Z.). Honglin Li is also sponsored by the National Program for Special Supports of Eminent Professionals and the National Program for Support of Top-Notch Young Professionals.

Supplementary materials

Supplementary material associated with this article can be found, in the online version, at doi:10.1016/j.cclet.2023.108825.

References

[1] J. Zhao, H. Zheng, Z. Sui, et al., Cytokine 123 (2019) 154726.
[2] Y. Ikeda, A. Murakami, H. Ohigashi, Mol. Nutr. Food Res. 52 (2008) 26–42.
[3] M.J. Tohme, M.C. Gimenez, A. Peralta, et al., Int. J. Antimicrob. Agents 54 (2019) 601–609.
[4] S. Xiao, Z. Tian, Y. Wang, et al., Med. Res. Rev. 38 (2018) 951–976.
[5] L. Kong, S. Li, Q. Liao, et al., Antiviral Res. 98 (2013) 44–53.
[6] S. Biswas, A. Kar, N. Sharma, et al., Ann. Med. 53 (2021) 2009–2017.
[7] Y. Jia, S. Kim, J. Kim, et al., Mol. Nutr. Food Res. 59 (2015) 344–354.
[8] X. Zhang, T. Li, E.S. Gong, R.H. Liu, J. Agric. Food Chem. 68 (2020) 7404–7415.
[9] V. Khwaza, O.O. Oyedeji, B.A. Aderibigbe, Int. J. Mol. Sci. 21 (2020) 5920.
[10] M.S. Jaman, M.A. Sayeed, Breast Cancer 25 (2018) 517–528.
[11] Z. Qian, X. Wang, Z. Song, et al., Biomed. Res. Int. 2015 (2015) 809714.
[12] Z. Zhu, Z. Qian, Z. Yan, et al., Int. J. Nanomed. 8 (2013) 129–136.
[13] X.H. Wang, S.Y. Zhou, Z.Z. Qian, et al., Exp. Opin. Drug Metab. Toxicol. 9 (2013) 117–125.
[14] H. Zhao, S. Tang, Q. Tao, et al., J. Agric. Food Chem. 71 (2023) 3981–3993.
[15] J. Shan, Y. Xuan, Q. Zhang, et al., Protein Cell 7 (2016) 571–585.
[16] S. Prasad, V.R. Yadav, B. Sung, et al., Clin. Cancer Res. 18 (2012) 4942–4953.
[17] Y.J. Zhang, S.F. Li, H. Zhang, H.W. Xu, Bioconjug. Chem. 32 (2021) 4–24.
[18] C. Zhou, J.Y. Zhang, H.B. Liu, et al., Eur. J. Med. Chem. 229 (2022) 114048.
[19] S. Chen, G. Dong, S. Wu, et al., Acta Pharm. Sin. B 9 (2019) 144–156.
[20] H. Yao, G. Wei, Y. Liu, et al., ACS Med. Chem. Lett. 9 (2018) 1030–1034.
[21] S. Xu, S. Luo, H. Yao, et al., J. Med. Chem. 59 (2016) 5022–5034.
[22] S...M. Deguire, D.C. Earl, Y. Du, et al., Angew. Chem. Int. Ed. 54 (2015) 961–964.
[23] R. Yamada, T. Takeshita, M. Hiraizumi, et al., Bioorg. Med. Chem. Lett. 24 (2014) 1839–1842.
[24] J. Wu, Q. Shen, Y. Wang, et al., ACS Med. Chem. Lett. 5 (2014) 911–914.
[25] P. Shaul, M. Frenkel, E.B. Goldstein, et al., ACS Med. Chem. Lett. 4 (2013) 323–328.
[26] G. Wells, M. Suggitt, M. Coffils, et al., Bioorg. Med. Chem. Lett. 18 (2008) 2147–2151.
[27] Y. Wu, Y. Zhang, X. Chen, et al., Eur. J. Med. Chem. 213 (2021) 113163.
[28] K.L. Li, S.C. Wu, G.P. Dong, et al., Chin. Chem. Lett. 34 (2023) 108231.
[29] M. Yang, S. Luo, X. Wang, et al., Front. Cell Dev. Biol. 9 (2021) 684526.
[30] J.R. Liang, E. Lingeman, T. Luong, et al., Cell 180 (2020) 1160–1177.
[31] H. Chino, N. Mizushima, Trends Cell Biol. 30 (2020) 384–398.
[32] A. Khaminets, T. Heinrich, M. Mari, et al., Nature 522 (2015) 354–360.
[33] D. Kashyap, H.S. Tuli, A.K. Sharma, Life Sci. 146 (2016) 201–213.
[34] M.H. Shyu, T.C. Kao, G.C. Yen, J. Agric. Food Chem. 58 (2010) 6110–6118.